Journal of Statistical Physics, Vol. 57, Nos. 3/4, 1989

Statistical Mechanics of Flux Lines in High-T_c Superconductors

David R. Nelson[1]

Received March 13, 1989

A theory of the entangled flux liquids which arise in the new high-T_c superconductors is reviewed. New physics appears because of the weak interplanar couplings and high critical temperatures in these materials. Flux line wandering melts the conventional Abrikosov flux lattice, and leads to an entangled vortex state whose statistical mechanics is closely related to the physics of interacting bosons in two dimensions. The phase diagram as a function of magnetic field and temperature is discussed, and it is argued that an entangled vortex liquid appears just above H_{c1} at all nonzero temperatures. The decay of vortex line correlations in the entangled liquid state is controlled by the superfluid excitation spectrum of the bosons. Line wandering produces drastic changes in the $B(H)$ constitutive relation near H_{c1}.

KEY WORDS: Superconductors; flux lines; bosons.

1. INTRODUCTION

One of the many fascinations of the CuO_2-based superconductors[1] is the possibility of novel fluctuations effects due to the high critical temperatures and small coherence lengths. Interesting modifications of the standard BCS-based Ginzburg–Landau mean-field theory may be expected at T_c in zero field,[2] and when the Abrikosov flux lattice forms with decreasing temperatures at H_{c2}.[3] Although fluctuations are usually limited to the immediate vicinity of critical points, it was recently argued that fluctuations in the high-T_c materials lead to a new entangled flux liquid *phase* in a magnetic field, due to flux line wandering as vortex filaments traverse the sample.[4,5]

[1] Lyman Laboratory of Physics, Harvard University, Cambridge, Massachusetts 02139.

0022-4715/89/1100-0511$06.00/0 © 1989 Plenum Publishing Corporation

There are now experiments indicating that the usual Abrikosov flux lattice is in fact melted over a significant portion of the (H, T) plane: Vibrating reed experiments of Gammel *et al.*[6] have found a striking signal suggestive of flux lattice melting in single crystals of $Bi_2Sr_2CaCu_2O_8$ (BSCCO) at temperatures well below the onset of the Meissner effect. Low-field flux-flow resistivity measurements (also on bismuth compounds) by van Dover *et al.*[7] show no threshold behavior for $T = 50$–80 K, indicative of vortices which flow freely without a shear modulus in the presence of weak pinning. These measurements are consistent with earlier observations: Although flux quanta (decorated via the Bitter technique) were observed emerging from a sample of $YBa_2Cu_3O_7$ (YBCO) at $T = 4.2$ K, no flux patterns could be discerned at $T = 77$ K, possibly due to time-dependent flux wandering in an equilibrated flux liquid.[8]

Melted flux liquids are already familiar from discussions of two-dimensional superconducting films: Dislocation-mediated melting (see, e.g., ref. 9) of the flux lattice leading to both ordinary and hexatic liquid phases of essentially point vortices was explored theoretically several years ago by Fisher.[10] The novelty of high-T_c superconductors lies in the possibility of a melted liquid of entangled *line* defects in three dimensions. It was argued in refs. 4 and 5 that the high-T_c materials are especially likely to exhibit an entangled liquid regime on the basis of an analogy with superfluidity of boson world lines in $2 + 1$ dimensions. A related analogy was proposed by Fisher and Lee,[11] who applied duality transformations to a lattice model of a superconductor. These theories also allow for a "disentangled flux liquid" regime, which would be the three-dimensional analogue of the liquid of point vortices discussed above.

In this paper I review these new theoretical developments. The starting point is the Gibbs free energy for N flux lines (see Fig. 1) whose positions

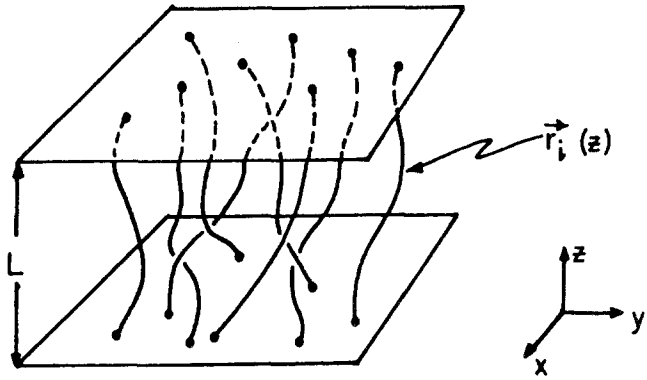

Fig. 1. Schematic of vortex lines in a slab of thickness L. The trajectory of the ith vortex along the z axis is described by the function $\mathbf{r}_i(z)$.

with a field **H** along the z direction (perpendicular to the CuO_2 planes) in a sample length L are given by $\mathbf{r}_i(z) = (x_i(z), y_i(z))$, $i = 1,..., N$. We work in the London limit, since the ratio of the penetration depth λ to the coherence length ξ is typically quite large, $\kappa = \lambda/\xi \approx 10^2$. If ε_1 is the energy per unit length of a single flux line, and $\phi_0 = 2\pi\hbar c/2e$ is the flux quantum, the energy reads[5]

$$G = \left(\varepsilon_1 - \frac{H\phi_0}{4\pi}\right) NL + \frac{\phi_0^2}{8\pi^2\lambda^2} \sum_{i>j} \int_0^L K_0\left(\frac{\mathbf{r}_{ij}(z)}{\lambda}\right) dz + \frac{1}{2}\tilde{\varepsilon}_1 \sum_{i=1}^{N} \int_0^L \left|\frac{d\mathbf{r}_i(z)}{dz}\right|^2 dz \tag{1}$$

where $\mathbf{r}_{ij} = \mathbf{r}_i - \mathbf{r}_j$ and $K_0(x)$ is the modified Bessel function, $K_0(x) \approx (\pi/2x)^{1/2} e^{-x}$ for large x. For an isotropic superconductor, the last term comes from the expansion of the total line energy, $E_i = \varepsilon_1 \int_0^L (1 + |d\mathbf{r}_i/dz|^2)^{1/2} dz$. In this case, $\tilde{\varepsilon}_1 = \varepsilon_1$. For the anisotropic layered compounds under consideration here, $\tilde{\varepsilon}_1$ is considerably smaller,[5]

$$\tilde{\varepsilon}_1 = \frac{M_\perp}{M_z} \varepsilon_1 \tag{2}$$

where $M_\perp$ is the in-plane effective mass, and $M_z \approx 10^2 M_\perp$ is the much larger effective mass describing the weak coupling between the planes. Conventional treatments of the transition at H_{c1} assume that the vortices form a triangular lattice of rigid rods with a real density $n = B/\phi_0$ parallel to the z axis, so that the last term of (1) vanishes. Flux lines begin to penetrate when the first term changes sign, i.e., when $H \geqslant H_{c1} = 4\pi\varepsilon_1/\phi_0$.

Balancing the first two terms then leads to[12,13]

$$B = \frac{2\phi_0}{3^{1/2}\lambda^2} \left\{\ln\left[\frac{3\phi_0}{4\pi\lambda^2(H - H_{c1})}\right]\right\}^{-2} \tag{3}$$

for H close to H_{c1}. Although this approximation works well for conventional superconductors, it fails in high-T_c materials due to the elevated temperatures and the small value of $\tilde{\varepsilon}_1$. I shall restrict attention here to single-crystal samples which are either sufficiently pure or at sufficiently high temperatures so that pinning by impurities can be neglected. Research on the effects of disorder is still rapidly developing, and is reviewed briefly in ref. 5.

A full statistical treatment of the partition function associated with Eq. (1) entails integration of $\exp(-G/k_B T)$ over all vortex trajectories $\{r_i(z)\}$. The partition function, for example, is

$$Z = \sum_{N=0}^{\infty} \frac{1}{N!} \int \mathscr{D}\mathbf{r}_1(z) \cdots \int \mathscr{D}\mathbf{r}_N(z) e^{-G/k_B T} \tag{4}$$

The Abrikosov mean-field theory which replaces flexible vortex lines by rigid rods is similar to the Frank–van der Meer theory of misfit dislocations near the commensurate–incommensurate transition in, e.g., krypton adsorbed on graphite. This zero-temperature theory becomes incorrect at finite temperatures due to dislocation line wandering.[14] We can estimate when the Abrikosov theory breaks down from a simple random walk argument.[4] We consider a single flux line $\mathbf{r}(z)$ and determine how far it wanders perpendicular to the z axis as it traverses the sample. The relevant path integral is

$$\langle |\mathbf{r}(z)-\mathbf{r}(0)|^2 \rangle = \frac{\int \mathscr{D}\mathbf{r}(s)\, |\mathbf{r}(z)-\mathbf{r}(0)|^2 \exp\left[-\dfrac{\tilde{\varepsilon}_1}{2k_B T}\displaystyle\int_0^L \left(\frac{d\mathbf{r}}{ds}\right)^2 ds \right]}{\int \mathscr{D}\mathbf{r}(s) \exp\left[-\dfrac{\tilde{\varepsilon}_1}{2k_B T}\displaystyle\int_0^L \left(\frac{d\mathbf{r}}{ds}\right)^2 ds \right]}$$

$$= \frac{2k_B T}{\tilde{\varepsilon}_1} |z| \tag{5}$$

which shows that the vortex "diffuses" as a function of the timelike variable z,

$$\langle |\mathbf{r}(z)-\mathbf{r}(0)|^2 \rangle^{1/2} = (2Dz)^{1/2} \tag{6}$$

with diffusion constant

$$D = \frac{k_B T}{\tilde{\varepsilon}_1} = \frac{M_\perp}{M_z} \frac{4\pi k_B T}{\phi_0 H_{c1}} \tag{7}$$

At $T = 77$ K, we take $H_{c1} \approx 10^2$ G and $M_z/M_\perp \approx 10^2$ and find $D = 10^{-6}$ cm, so that vortex lines wander a distance of order 1 um while traversing a sample of thickness 0.01 cm.

These close encounters will occur quite frequently in fields of order 10–100 KG, where vortices are separated by distances of order 500 Å or less. Collisions between neighboring vortices must now be taken into account. As shown in ref. 4, this effect dominates the weak repulsive interaction in Eq. (1) close to H_{c1} in sufficiently thick samples. More generally, we can define an "entanglement correlation length"

$$\xi_z \equiv \frac{1}{2Dn} = \frac{\tilde{\varepsilon}_1}{2k_B T n} \tag{8}$$

which is the spacing between collisions in a vortex liquid areal density $n = B/\phi_0$. Collisions and entanglement of vortex lines will significantly alter the Abrikosov theory whenever

$$L \gg \xi_z \tag{9}$$

2. ANALOGY WITH BOSON STATISTICAL MECHANICS IN TWO DIMENSIONS

It is not hard to show that the transfer matrix connecting neighboring constant-z slices of the partition function (4) is just the exponential of the N-particle Hamiltonian operator in imaginary time for quantum mechanical particles interacting with a potential proportional to $K_0(r/\lambda)$. Indeed, Eq. (4) is just the imaginary-time Feynman path integral[15] for this problem with free boundary conditions for the particle world lines. The statistical mechanics as $L \to \infty$ will be dominated by the ground-state wave function. Although there is no *a priori* requirement that the solutions of this Schrödinger equation obey boson or fermion statistics, one can show quite generally that the *ground state* wave function is bosonic.[15]

To extend this analogy to finite L, it is helpful to first consider the special experimental geometry with a toroidal magnetic field shown in Fig. 2. The vortex trajectories $\{\mathbf{r}_i(s)\}$ are now functions of arc length s around the torus instead of z. The partition function differs from Eq. (4) in that we must now impose periodic boundary conditions on the vortex lines: a configuration of vortices in any given circular cross section must return to itself when the vortex lines are followed around the torus. To completely sample the allowed phase space, we must sum over different ways of connecting the vortices as they traverse the circuit. The partition function (4) is replaced by

$$Z' = \sum_{N=0}^{\infty} \frac{1}{N!} \sum_{P} \int_{\mathbf{r}_1(L)=P[\mathbf{r}_1(0)]} \mathscr{D}\mathbf{r}_1(s) \cdots \times \int_{\mathbf{r}_N(L)=P[\mathbf{r}_N(0)]} \mathscr{D}\mathbf{r}_N(s) e^{-G/k_BT} \tag{10}$$

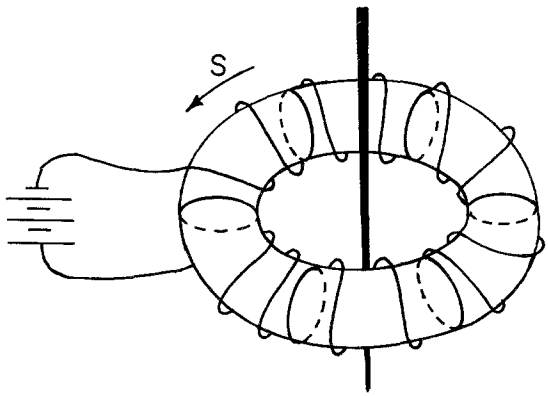

Fig. 2. Toroidal superconducting sample in a toroidal magnetic field for which the analogy with the statistical mechanics of two-dimensional bosons becomes exact.

where we have imposed periodic boundary conditions and summed over permutations P in contrast to the free boundary conditions implicit in (4). The parameter s runs from zero to L, where L is the average circumference around the torus. The effects of inhomogeneities in this circumference, as well as of inhomogeneities in the magnetic field, are discussed in ref. 5.

As given by Eq. (10), the partition function is identical to the imaginary-time Feynman path integral[15] for the grand canonical partition function of a fluid of interacting bosons in two dimensions with chemical potential $\mu = H\phi_0/4\pi - \varepsilon_1$. The trajectories of vortices around the torus are isomorphic to boson world lines. The thermal energy $k_B T$ plays the role of $\hbar$, while the circumference L corresponds to the distance $\beta\hbar$ in the imaginary time direction. The parameter $\tilde{\varepsilon}_1$ plays the role of the boson mass. This analogy, which is summarized in Table I, clearly shows why vortex lines are interesting in high-T_c superconductors: these materials allow us to explore a world of exceptionally light ($\tilde{\varepsilon}_1 \ll \varepsilon_1$) bosons in which "Planck's constant" (i.e., $k_B T$) is ten times larger than in conventional materials. Because $\tilde{\varepsilon}_1$ tends to zero as $T \to T_c$ along the H_{c1} curve[12,13], the boson "mass' can be made arbitrarily small. The importance of vortex line fluctuations is determined in the boson language by the "thermal de Broglie wavelength" Λ_L, which translates according to Table I into

$$\Lambda_L \equiv \left(\frac{2\pi\hbar^2\beta}{m}\right)^{1/2} = \left(\frac{2\pi k_B T L}{\tilde{\varepsilon}_1}\right)^{1/2} \tag{11}$$

Except for numerical factors, this is the vortex diffusion distance (6) with $z = L$. Quantum fluctuations begin to become important for bosons when $\Lambda_L \gtrsim n^{-1/2}$. They dominate the physics for $\Lambda_L \gg n^{-1/2}$, which is equivalent to Eq. (9).

Figure 3 shows the expected phase diagram for two-dimensional bosons as a function of "chemical potential" $(H - H_{c1})$ and "temperature" (L^{-1}). The real temperature is held fixed at $T < T_c$. A liquid–gas critical point is absent, because we have assumed a purely repulsive pair potential.

Table I. Detailed Correspondence of the Parameters of Melted Flux Liquid with the Mass, Value of Planck's Constant, Reciprocal Temperature β, and Potential of Two-Dimensional Bosons

Vortex lines	$\tilde{\varepsilon}_1$	$k_B T$	L	$H\phi_0/4\pi - \varepsilon_1$	$(\phi_0^2/8\pi^2\lambda^2)\, K_0(r/\lambda)$
Two-dimensional Bosons	m	$\hbar$	$\beta\hbar$	μ	Boson pair Potential

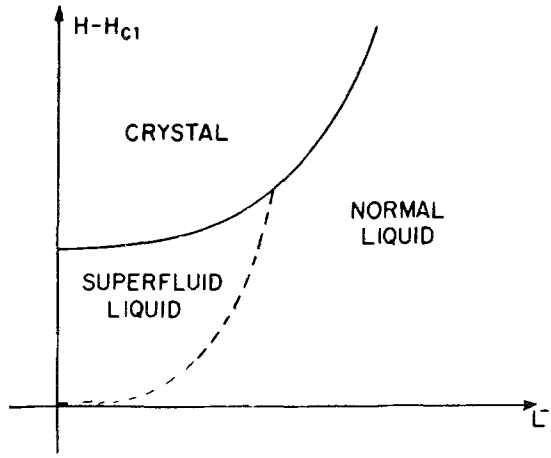

Fig. 3. Schematic phase diagram for vortex lines in a toroidal geometry as a function of "chemical potential" $H - H_{c1}$ and "temperature" L^{-1}. Here, L is the average circumference of the torus in Fig. 2.

The meaning of the "crystalline," "normal liquid," and "superfluid liquid" phases for Abrikosov flux lines is illustrated schematically in Fig. 4. The large dots show where the vortex lines pierce, say, the $s = 0$ circular cross section of the torus in Fig. 2. The lines show the vortex positions in subsequent cross sections as they traverse the interior of the torus and return to the initial cross section. Figure 4a represents a toroidal Abrikosov flux lattice, in which the vortices typically make only small excursions from the sites of a triangular lattice. Figure 4b represents a disentangled flux liquid characterized by somewhat larger excursions of the vortices and no crystalline order in their average positions. In this case, the torus is filled with a liquid of disconnected flux bracelets. Figure 4c represents an *entangled* flux liquid in which vortices repeatedly exchange places in a complicated dance as they traverse the torus.

The elegant picture[15] of a superfluid liquid embodied in Fig. 4c has been confirmed in some striking computer simulations of Ceperley and Pollock in both two and three dimensions.[16] The beauty of the high-T_c superconductors is that Feynman's artificial imaginary time variable becomes real and directly accessible to experiments. In its entangled "superfluid" phase, the flux liquid in a torus looks like a mangled spiral of flux lines which makes many turns around the torus before repeating itself. A finite fraction of the vortex loops are connected together in such long cycles, which should have important consequences for flux flow resistivity in the presence of a dilute concentration of pinning centers. The dashed curve in Fig. 3 is a line of Kosterlitz–Thouless transitions from an

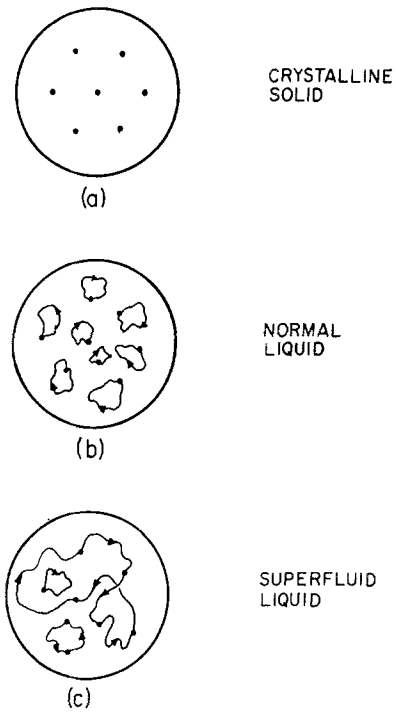

Fig. 4. Trajectories $\mathbf{r}_i(s)$ swept out by vortex lines within a circular cross section of the torus in Fig. 2. All vortices occupy approximately the same relative position within the cross section for all values of s within the Abrikosov flux lattice phase (a). These lines form disentangled flux bracelets in the normal liquid phase, but may wander appreciably during their circuit around the torus, as shown in (b). In superfluid phase (c), the flux lines link up, and it may require many circuits around the torus before a flux line returns to its starting point.

entangled flux liquid to a disentangled one. Flux flow resistivity will be suppressed in an entangled flux liquid with a few strong pinning centers, even though there is no shear modulus.

Figure 5 shows the Abrikosov flux lattice, the disentangled flux liquid, and the entangled flux liquid as they would appear in a conventional experimental geometry, with free boundary conditions on the vortex lines. As discussed above, boundary conditions should be irrelevant as the sample thickness tends to infinity. It can be shown[5] that the entangled flux liquid is indistinguishable from a "superfluid" with periodic boundary conditions whenever (9) is satisfied. It is possible, however, that the Kosterlitz–Thouless transition discussed above is smeared out with free boundary conditions, as suggested by Fisher and Lee.[11] It may then be

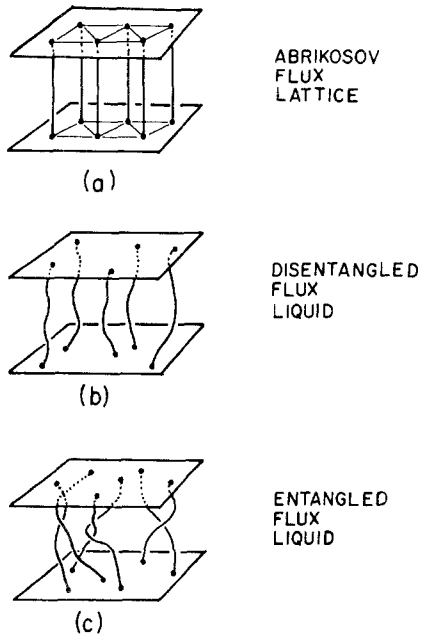

Fig. 5. Analogues of the three phases shown in Fig. 6 for a slab geometry with free, rather than periodic boundary conditions. In contrast to the case of periodic boundary conditions, there is not necessarily a sharp phase transition between (b) and (c).

better to speak of entangled an disentangled flux liquid *regimes* instead of phases.[2] The crossover between these two regimes will occur when

$$\xi_z \approx L \tag{12}$$

i.e., when the "thermal de Broglie wavelength" Λ_L is comparable to the vortex line spacing.[4]

3. PHASE DIAGRAMS

I have argued that flexible vortex lines can exist in crystalline, entangled flux liquid, or disentangled flux liquid states. I now discuss where these phases may be expected to occur in the (H, T) phase diagram in

[2] Note, however, that this issue is not yet settled in the closely related problem of entangled polymer melts, where there may actually be a phase transition as a function of the polymerization index N.[17] There are, moreover, subtle effects associated with topological entanglement of interacting line defects special to $2+1$ dimensions; these have no analogue in higher dimensions, where braided world lines can always disentangle.

typical high-T_c materials. I shall focus primarily on samples whose thickness L in the field direction is large, so that only the crystalline and entangled flux liquid phases need to be considered (see Fig. 3). The melting of the flux lattice will be discussed in terms of the Lindemann criterion. I point out that the Lindemann criterion becomes invalid at sufficiently small fields, and argue that a melted flux liquid will always exists at any finite temperature sufficiently close to H_{c1}.[4]

3.1. Continuum Elastic Theory and the Lindemann Criterion

To discuss melting of a triangular flux lattice, we assume that the external field is aligned with the z direction, and describe the trajectory of the ith vortex by a function $\mathbf{r}_i(z)$. If the average position of the ith vortex in the triangular lattice discussed above is denoted by $\mathbf{R}_i$, we can define a two-dimensional displacement field $\mathbf{u}(\mathbf{R}_i, z)$ by

$$\mathbf{r}_i(z) = \mathbf{R}_i + \mathbf{u}(\mathbf{R}_i, z) \tag{13}$$

In the continuum limit, this displacement becomes a function $\mathbf{u} = \mathbf{u}(x, y, z)$. The excess free energy $\delta\mathbf{G}\{\mathbf{u}(\mathbf{r})\}$ associated with small gradients of $\mathbf{u}$ is[18]

$$\delta G\{\mathbf{u}(\mathbf{r})\} = \frac{1}{2}\int d^3r \left[2\mu u_{\alpha\beta}^2 + \lambda u_{\delta\delta}^2 + K\left(\frac{\partial \mathbf{u}}{\partial z}\right)^2 \right] \tag{14}$$

where

$$u_{\alpha\beta}(\mathbf{r}) = \frac{1}{2}\left(\frac{\partial u_\alpha}{\partial r_\beta} + \frac{\partial u_\beta}{\partial r_\alpha}\right), \qquad \alpha, \beta = x, y \tag{15}$$

is the symmetrized two-dimensional strain matrix, μ and λ are Lamé coefficients, and K is a tilt elastic constant.

As pointed out by de Gennes and Matricon, two constraints on these three elastic constants are provided by the macroscopic magnetic properties of the material. The bulk modulus of the line lattice is[18]

$$\mu + \lambda \approx \frac{B^2}{4\pi} \tag{16}$$

More generally, the sum $\mu + \lambda$ is given by $\mu + \lambda = B_0^2/4\pi\mu_z$, where $\mu_z = dB(H)/dH$ is the longitudinal magnetic permeability.

For isotropic superconductors, the tilt modulus is[18]

$$K = \frac{HB}{4\pi} \tag{17}$$

The tilt modulus will be much smaller, however, for anisotropic high-T_c superconductors with weakly coupled planes. For $\mathbf{H} \| \hat{z}$, a reasonable guess is[5]

$$K \approx \frac{M_\perp}{M_z} \frac{HB}{4\pi} \tag{18}$$

Note that K vanishes as M_z^{-1} for large M_z, as is physically reasonable when the coupling between CuO_2 planes tends to zero. If the ratio $M_\perp/M_z$ is estimated from the upper critical fields parallel and perpendicular to the z axis $[M_\perp/M_z = (H_{c2}^{\parallel}/H_{c2}^{\perp})^2]$, one finds $M_\perp/M_z 10^{-2}$. The tilt modulus is clearly bounded above by the isotropic result (17). For $H \gg H_{c1}$, we can set $B = H$ in (18).

The only elastic constant not determined directly by the magnetic properties is the shear modulus. The shear modulus is much smaller than the bulk modulus for most regimes of interest, and actually vanishes near H_{c2}, as shown by Labusch[19]

$$\mu \approx 7 \times 10^{-3} \left(\frac{H_{c2}}{\kappa}\right)^2 \left(\frac{1 - H}{H_{c2}}\right)^2 \tag{19}$$

We can use (19) to approximate μ for $\frac{1}{2}H_{c2} \lesssim H \leq H_{c2}$. For the opposite limit of $H_{c1} \leq H \lesssim \frac{1}{2}H_{c2}$, we can use[5] the result of Fetter *et al.*[20],

$$\mu \approx \frac{1}{4} \frac{B\phi_0}{(4\pi\lambda)^2} \tag{20}$$

These are zero-temperature results for shear distortions of triangular Abrikosov lattices with flux lines regarded as rigid rods. At finite temperatures, the random-walk-like vortex fluctuations discussed elsewhere in this review can produce (potentially important) renormalizations of both the shear and the tilt moduli.

We are now in a position to estimate the mean-square displacement of a flux line, i.e.,

$$\begin{aligned} \langle |\mathbf{u}(\mathbf{r}_0)|^2 \rangle &= \frac{\int \mathscr{D}\mathbf{u}(\mathbf{r})\, |\mathbf{u}(\mathbf{r}_0)|^2\, e^{-\delta G/k_B T}}{\int \mathscr{D}\mathbf{u}(\mathbf{r}) e^{-\delta G/k_B T}} \\ &= \int \frac{d^3q}{(2\pi)^3} \left[\frac{k_B T}{\pi q_\perp^2 + K q_z^2} + \frac{k_B T}{(2\mu + \lambda) q_\perp^2 + K q_z^2} \right] \end{aligned} \tag{21}$$

where $q_\perp^2 = q_x^2 + q_y^2$. We take the cutoff to infinity in the z direction, and impose for simplicity a circular cutoff Λ in the (x, y) plane. We choose

$A = (4\pi n)^{1/2}$, where n is the vortex line density, which conserves the area of the hexagonal Brillouin zone. The mean-square displacement is then

$$\langle |\mathbf{u}(\mathbf{r}_0)|^2 \rangle = \left(\frac{n}{4\pi}\right)^{1/2} \left[\frac{k_B T}{(\mu K)^{1/2}} + \frac{k_B T}{[(2\mu + \lambda)K]^{1/2}} \right] \tag{22}$$

Because the shear modulus tends to zero at H_{c2}, $\langle |\mathbf{u}(\mathbf{r})|^2 \rangle$ diverges in this approximation, suggesting that the Abrikosov flux lattice may melt, as originally pointed out by Labusch.[19] The shear modulus is small relative to the bulk modulus at all fields, so we can always neglect the second term in Eq. (22). Upon inserting the estimates (19) and (18) for μ and K, we find

$$\begin{aligned} \langle |\mathbf{u}(\mathbf{r})|^2 \rangle &\approx \left(\frac{n}{4\pi K u}\right)^{1/2} k_B T \\ &\approx (12\kappa k_B T) \left(\frac{M_z}{M_\perp \phi_0^3 H_{c2}}\right)^{1/2} \frac{h^{1/2}}{(1-h)} d^2 \end{aligned} \tag{23}$$

where $d \approx (\phi_0/B)^{1/2}$ is the spacing between vortex lines, and the reduced field $h = H/H_{c2}$.

Taking as parameters for BSCCO $\kappa = 2 \times 10^2$, $H_{c2}(T = 77\ K) = 2 \times 10^4$ Oe, and $(M_z/M_\perp)^{1/2} = 15$, we find that the root-mean-square fluctuation in the line displacement at liquid nitrogen temperatures is

$$\langle |\mathbf{u}|^2 \rangle^{1/2} \approx 0.2 \frac{h^{1/4}}{(1-h)^{1/2}} d \tag{24}$$

Since most solids melt when the rms displacement becomes of order 1/10 of the interparticle spacing, the flux lattice in the BSCCO compounds should indeed be melted for a wide range of fields,[8] at least for $\mathbf{H} \| \hat{z}$. Inserting parameters for YBCO suggests that it will be necessary to take H considerably closer to H_{c2} to obtain melting,[5] again in accordance with experiment.[8]

Although these results are encouraging, it is worth pointing out that the Lindemann condition is a *criterion*, and not a *theory* of melting. It does not attempt to explain the melting mchanism in detail, nor does it provide an explanation of the apparently continuous changes during melting observed by Gammel *et al.*[8] As discussed above, the Lindemann criterion assumes wave vector-independent elastic constants, which can be a gross oversimplification, especially if fluctuations are important. The integral in (21) is in fact dominated by $q \sim 1/d$. A more accurate theory would use wave vector-dependent elastic constants under the integral sign in Eq. (21).[5] This has been done by Houghton *et al.*,[21] who generalize nonlocal elastic constants derived by Brandt and Essman.[22] As pointed out by

Houghton *et al.*, there are significant corrections to the Lindemann criterion due to model effects in high-T_c materials unless H is fairly small. These nonlocal effects act to *enhance* the fluctuation-induced melting considered above. By using the Lindemann ratio as a fitting parameter (they find $\langle u^2 \rangle^{1/2} = 0.4d$ at melting), these authors are able to obtain good fits to the melting curves of ref. 6 for both YBCO and BSCCO.

3.2. Shape of the Melting Curve Near H_{c1}

The Lindemann analysis sketched above cannot be correct in the vicinity of H_{c1}, i.e., when the flux line spacing is of order the London penetration depth or more. This is the regime of most flux decoration experiments.[8] The classical theory, based on energetic considerations alone, predicts that $\mu \sim \lambda \sim \exp(-d/\lambda)$ as the vortex separation $d \to \infty$.[22] There are, however, important entropic effects due to flux line wandering which dominate over flux line interaction energies in the dilute limit. In this section, I show that these entropy effects always destabilize the flux lattice relative to an entangled flux liquid sufficiently close to H_{c1}.[4] This result is implicit in Fig. 3, where a "superfluid" (i.e., entangled flux liquid) phase exists over a range of $H - H_{c1}$ values when $L = \infty$. Zero-point motion always melt boson crystals with a purely repulsive pair potential (provided it falls off faster than $1/r^2$) in the dilute limit.[3]

As discussed in the Introduction, collisions between vortex lines are important whenever Eq. (9) is satisfied. In the crystalline phase, each line will typically wander until it is reflected backward by a collision with one of its six near neighbors. Taking over the argument of Coppersmith *et al.* for domain walls in two dimensions,[14] we note that each collision reduces the entropy in the partition function (4) relative to a noninteracting system by $k_B \ln q$, with $q > 1$. Here, q is the amount by which the number of choices available to the random walking flux line is reduced by each collision. If the set of allowed vortex positions in each constant-z cross section is assumed for simplicity to be a fine mesh triangular lattice, one might take, e.g., $q = 6/3 = 2$. Since the spacing ξ_z between collisions in the z direction is given by Eq. (8), the total number of collisions in a sample of thickness L is of order $(L/\xi_z)N \sim (LA)\, n^2 k_B T/\tilde{\varepsilon}_1$, where A is the cross-sectional area. As a result, the statistically averaged Gibbs free energy per unit volume of the crystal acquires an entropic contribution proportional to n^2,[4]

$$g_{\text{crystal}}(n) = (\varepsilon_1 - H\phi_0/4\pi)n + (3\phi_0^2/8\pi^2\lambda^2)\, K_0(d/\lambda)n + (k_B T)^2\, n^2 (\ln q)/\tilde{\varepsilon}_1 \tag{25}$$

[3] See ref. 23 for explicit calculations for a quantum boson solid with a Yukawa potential in *three* dimensions.

Only the contribution from the six nearest neighbors has been used to estimate the second term of (25). Because $K_0(d/\lambda) \sim \exp(-d/\lambda)$ as $d \sim n^{-1/2} \to 0$, we can neglect the energetic contribution to (25) and write (upon setting $H_{c1} = 4\pi\varepsilon_1/\phi_0$)

$$g_{\text{crystal}}(n) = -\frac{\phi_0}{4\pi}(H - H_{c1})n + \frac{(k_B T)^2 \ln q}{\tilde{\varepsilon}_1} n^2 + \cdots \tag{26}$$

Upon minimizing with respect to n, we find that the density of lines in the flux crystal is

$$n = \frac{B}{\phi_0} \approx \frac{\phi_0 \tilde{\varepsilon}_1}{8\pi \ln q}\left(\frac{1}{k_B T}\right)^2 (H - H_{c1}) \tag{27}$$

and that the crystalline free energy is

$$g_{\text{crystal}} = -\frac{\phi_0^2 \tilde{\varepsilon}_1}{(8\pi k_B T)^2}\frac{(H - H_{c1})^2}{\ln q} \tag{28}$$

The same result can be obtained using the analogy with two-dimensional bosons described in Section 2: the term proportional to n^2 in Eqs. (25) and (26) arises from the zero-point energy of a quantum solid.

Because the entangled flux liquid phase corresponds to a Bose superfluid, we can obtain its free energy using results for two-dimensional bosons with a repulsive potential. The ground-state energy per particle is known to be [24]

$$\frac{E}{N} = \left(\frac{2\pi\hbar^2}{m}\right)\frac{n}{\ln(1/n\lambda^2)}\left[1 + O\left(\frac{1}{\ln(1/n\lambda^2)}\right)\right] \tag{29}$$

where n is the boson number density and λ is the interaction range. Upon constructing the free energy per unit area

$$g_{\text{liquid}} = (E - \mu N)/A \tag{30}$$

and transcribing the results into the language of high-temperature superconductors using Table I, we find that the energy of the entangled flux liquid is

$$g_{\text{liquid}} = -\frac{\phi_0}{4\pi}(H - H_{c1})n + \frac{2\pi(k_B T)^2}{\tilde{\varepsilon}_1}\frac{n^2}{\ln(1/n\lambda^2)} + \cdots \tag{31}$$

Minimizing with respect to n gives a flux line density[4]

$$n = \frac{B}{\phi_0} \approx \frac{\phi_0 \tilde{\varepsilon}_1}{(4\pi k_B T)^2}(H - H_{c1}) \ln\left[\left(\frac{4\pi k_B T}{\lambda}\right)^2 \frac{1}{\tilde{\varepsilon}_1 \phi_0 (H - H_{c1})}\right] \tag{32}$$

and a free energy

$$g_{\text{liquid}} \simeq -\frac{\phi_0^2 \tilde{\varepsilon}_1}{8\pi(4\pi k_B T)^2}(H-H_{c1})^2 \times \ln\left[\left(\frac{4\pi k_B T}{\lambda}\right)^2 \frac{1}{\tilde{\varepsilon}_1 \phi_0 (H-H_{c1})}\right] \tag{33}$$

Because of the logarithmic dependence on $H-H_{c1}$ in (33), the *free energy of the entangled liquid is always lower than that of the crystal in the dilute limit.* The transition between these two states occurs when the free energies are equal, i.e., at a field $H_x(T)$, which we readily find to be given by

$$\delta h_x \equiv \frac{H_x - H_{c1}}{H_{c1}} \approx \text{const} \times \left(\frac{k_B T}{\lambda}\right)^2 \frac{1}{\varepsilon_1 \tilde{\varepsilon}_1} \tag{34}$$

The width of the entangled flux liquid phase rises like T^2 at low temperatures. An analogous sliver of melted domain wall liquid appears between the commensurate and incommensurate phases in $1+1$ dimensions.[14] Because[12,13] $\varepsilon_1 = (4\pi\phi_0/\lambda^2)\ln\kappa$, we can rewrite (34) as

$$\delta h_x = \text{const} \times \left(\frac{k_B T \lambda}{4\pi\phi_0 \ln\kappa}\right)^2 \frac{\varepsilon_1}{\tilde{\varepsilon}_1} \tag{35}$$

which shows that the region occupied by the entangled flux liquid becomes large when the London penetration depth diverges $[\lambda \sim 1/(T_c - T)^{1/2}]$ near T_c.

Figure 6 shows schematic phase diagrams for BSCCO and YBCO, which combine the high-field Lindemann criterion melting curves of Houghton *et al.*[21] with the low-field estimate of the melting curve discussed above.[4] This phase diagram corrects an early guess[4] which did not account for the Lindemann criterion[5,21] and which incorrectly showed a finite range of entangled flux liquid at $T=0$. The field is assumed to be perpendicular to the CuO_2 planes. The region occupied by the entangled flux liquid is much larger for BSCCO, because $M_z/M_\perp$ is much larger in this case. For most conventional superconductors, the reentrant melting curve $H_x(T)$ is indistinguishably close to $H_{c1}(T)$ and $H_{c2}(T)$. The sliver of melted flux liquid close to H_{c1} may be difficult to observe even in the high-T_c materials. The mean-field transition line at H_{c2} need not be a sharp

[4] Phase diagrams similar to those in Fig. 6 have also been constructed by D. Huse.[25] I am indebted to Dr. Huse for pointing out that one cannot simply set $\tilde{\varepsilon}_1 = (M_\perp/M_z)\varepsilon_1$ in Eqs. (34) and (35), because of residual electromagnetic couplings between vortices which invalidate Eq. (2) in the dilute limit. As Huse has shown, $\tilde{\varepsilon}_1$ is of order ε_1 in this limit. For a discussion of this electromagnetic coupling in conventional superconductors (the DC transformer effect), see Ref. (26).

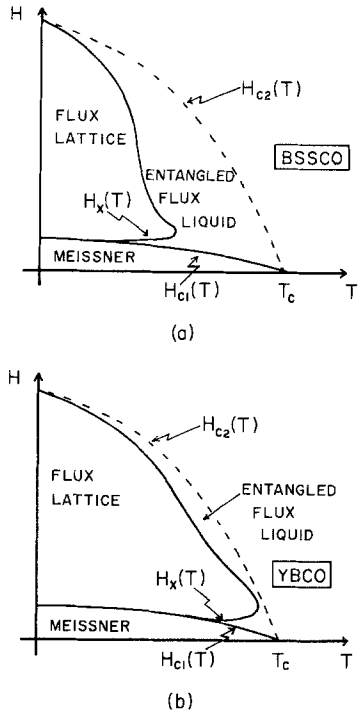

Fig. 6. Schematic phase diagrams for thick ($L \gg \xi_z$) single-crystal samples of (a) BSSCO and (b) YBCO for magnetic fields **H** directed perpendicular to the CuO_2 planes. The Meissner, Abrikosov flux lattice, and entangled flux liquid phases are shown. The melting curve $H_x(T)$ was obtained by combining the Lindemann criterion calculations of Houghton *et al.*[21] with the low-field result, Eq. (34). A thin sliver of entangled flux liquid phase is interposed between the Meissner and Abrikosov flux lattice phases at all nonzero temperatures. The curve $H_{c2}(T)$, which need not be a sharp phase transition, marks the onset of the Meissner effect.

phase transition when fluctuations are taken into account[10,11]; experimentally, it is defined by the onset of an (incomplete) Meissner effect with decreasing temperatures. We have not considered the possibility of an (possibly entangled) hexatic phase[9,10] in this analysis. There can also be modifications due to the finite sample size L along the z direction. Strictly speaking, $H_{c1} = 0$ for finite thickness films.[10] Equation (12), with $\xi_z = \tilde{\varepsilon}_1/2k_B Tn$, defines a locus in the melted portion of the phase diagram separating disentangled from entangled flux liquid regimes. In the thermodynamic limit $L \to \infty$, however, the melted liquid is always entangled.

4. PROPERTIES OF THE ENTANGLED FLUX LIQUID

The entangled flux liquid is a new phase of matter of substantial interest in its own right. Of particular interest is the vortex line correlation

function, which can be measured with neutron scattering.[27] These experiments measure fluctuations in the local density of flux lines, defined by

$$n(\mathbf{r}_\perp, z) = \sum_{i=1}^{N} \delta[\mathbf{r}_\perp - \mathbf{r}_i(z)] \tag{36}$$

Neutron scattering measures

$$\hat{S}(\mathbf{q}_\perp, q_z) = \langle |n(\mathbf{q}_\perp, q_z)|^2 \rangle \tag{37}$$

where $n(\mathbf{q}_\perp, q_z)$ is the Fourier transform of $n(\mathbf{r}_\perp, z)$. The physics, however, is more conveniently discussed in terms of the partial Fourier transform

$$\begin{aligned} S(\mathbf{q}_\perp, z) &= \int_{-\infty}^{\infty} \frac{dq_z}{2\pi} e^{-iq_z z} \hat{S}(\mathbf{q}_\perp, q_z) \\ &= \langle n(\mathbf{q}_\perp, z + z_0)\, n_\perp^*(\mathbf{q}_\perp, z_0) \rangle \end{aligned} \tag{38}$$

As illustrated in Fig. 7a, this correlation function reduces to the structure function of a cross section of the vortex lines when $z = 0$. The correla-

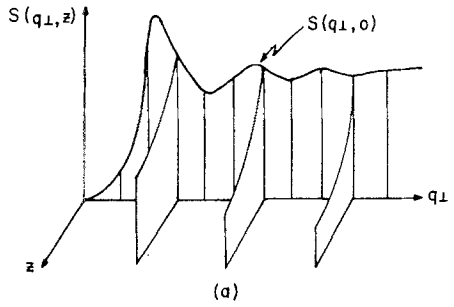

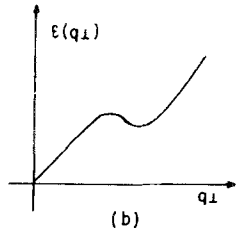

Fig. 7. (a) Partial structure function $S(\mathbf{q}_\perp, z)$ for an entangled liquid of vortex lines. For $z = 0$, this quantity is just the Fourier transform of the distribution of vortices in a constant-z cross section. $S(\mathbf{q}_\perp, z)$ decays exponentially with z. (b) Boson single-particle excitation spectrum which controls the decay of the $z = 0$ Fourier components in Fig. 2b according to Eq. (39).

tions in any such constant-z cross section should be similar to those of a two-dimensional liquid. Equation (38) describes more generally how the Fourier components of this $2D$ structure function decay along the z axis due to entanglement. As shown in ref. 5, this decay can be approximated by

$$S(\mathbf{q}_\perp, z) \approx S(\mathbf{q}_\perp, z=0) e^{-\varepsilon(q_\perp)|z|/k_B T} \tag{39}$$

where $\varepsilon(q_\perp)$ is the excitation spectrum of the corresponding superfluid (see Fig. 7b). Although these calculations were carried out using approximations suitable for a dilute gas of vortex lines, both the structure factor and excitation spectrum in Fig. 7 are sketched as one would expect them to be for heavily entangled flux liquid. Equation (39) corresponds to the "single-mode" approximation for superfluid dynamics. The excitation spectrum defines via Eq. (39) a $q_\perp$-dependent correlation length

$$\xi_\parallel(q_\perp) \equiv k_B T/\varepsilon(q_\perp) \tag{40}$$

The quantity $\xi_\parallel(q_\perp)$ is of the order of the entanglement correlation length ξ_z [see Eq. (8)] when $q_\perp \sim 1/d$, where d is an intervortex spacing.[5]

It is also possible to derive the $B(H)$ constitutive relation near H_{c1} [i.e., Eq. (32)] directly without appealing to the analogy with a dilute bose gas.[5] Equation (32) may be rewritten as

$$B(H) \approx \frac{\tilde{v}}{4\pi}(H - H_{c1}) \ln\left[\frac{4\pi}{\tilde{v}} \frac{(\phi_0/\lambda^2)}{H - H_{c1}}\right] \tag{41}$$

where the key dimensionless parameter in the theory is

$$\tilde{v} = \frac{\tilde{\varepsilon}_1 \phi_0^2}{4\pi (k_B T)^2} \tag{42}$$

Although the parameter $\tilde{\varepsilon}_1$ is small ($\tilde{\varepsilon}_1 \ll \varepsilon_1$) over much of the (H, T)-plane, as pointed out by D. Huse,[4] it becomes of order ε_1 near H_{c1}. There is also a logarithmic divergence in the specific heat as H approaches H_{c1} from above.[4] The coefficient of the divergence can be obtained by differentiating Eq. (33) with respect to temperature. The lower critical field itself is renormalized downward by fluctuations.[5]

Our understanding of flux lines in high-temperature superconductors is developing rapidly on both the theoretical and experimental fronts. Much theoretical work remains to be done. I have not even discussed the statics and dynamics of flux lines in the presence of random pinning centers, a subject which is discussed briefly in ref. 5. Of particular interest

in this regard is early work by Wördenweber and Kes and by Brandt on "dimensional crossover" in flux pinning, which suggests an entangled spaghettilike state due to pinning centers in thick samples even in the absence of thermal fluctuations.[28]

ACKNOWLEDGMENTS

It is a pleasure to dedicate this review to E. D. G. Cohen. Much of the theoretical discussion here is extracted from refs. 4 and 5. I am indebted to H. Sebastian Seung for the collaboration which led to ref. 5, and to R. A. Pelcovits for sending me ref. 21 prior to publication. During the course of this research I benefitted from conversations with D. J. Bishop, D. Ceperley, R. B. van Dover, P. L. Gammel, P. Ginzparg, B. I. Halpering, D. Huse, M. Kardar, R. S. Markiewicz, P. C. Martin, I. Silvera, and M. Tinkham. This work was supported by the National Science Foundation through grant DMR-8817291 and through the Harvard Materials Research Laboratory.

REFERENCES

1. M. Rice, *Z. Phys. B* **67**:141 (1987), and references therein.
2. C. Dasgupta and B. I. Halperin, *Phys. Rev. Lett.* **47**:1556 (1981).
3. E. Brézin, D. R. Nelson, and A. Thiaville, *Phys. Rev. B* **31**:7124 (1985).
4. D. R. Nelson, *Phys. Rev. Lett.* **60**:1973 (1988).
5. D. R. Nelson and H. S. Seung, *Phys. Rev. B* **39**:9153 (1989).
6. P. L. Gammel, L. F. Schneemeyer, J. V. Waszczak, and D. J. Bishop, *Phys. Rev. Lett.* **61**:1666 (1988).
7. R. B. van Dover, L. F. Schneemeyer, E. M. Gyorgy, and J. V. Waszczak, *Phys. Rev. B* (in press).
8. P. L. Gammel, D. J. Bishop, G. J. Dolan, J. R. Kwo, C. A. Murray, L. F. Schneemeyer, and J. V. Waszczak, *Phys. Rev. Lett.* **59**:2592 (1987).
9. D. R. Nelson, in *Phase Transitions and Critical Phenomena*, Vol. 7, C. Domb and J. L. Lebowitz, ed. (Academic, New York, 1983), p. 1.
10. D. S. Fisher, *Phys. Rev. B* **22**:1190 (1980).
11. M. P. A. Fisher and D. H. Lee, *Phys. Rev. B* **39**:2756 (1989).
12. A. L. Fetter and P. C. Hohenberg, in *Superconductivity*, Vol. 2, R. D. Parks, ed. (Dekker, New York, 1969).
13. M. Tinkham, *Introduction to Superconductivity* (McGraw-Hill, New York, 1975).
14. S. N. Coppersmith, D. S. Fisher, B. I. Halperin, P. A. Lee, and W. F. Brinkman, *Phys. Rev. B* **25**:349 (1982); J. Villain and P. Bak, *J. Phys.* **42**:657 (1981).
15. R. P. Feynman and A. R. Hibbs, *Quantum Mechanics and Path Integrals* (McGraw-Hill, New York, 1965); R. P. Feynman, *Statistical Mechanics* (W. A. Benjamin, Reading, Massachusetts, 1972).
16. D. M. Ceperley and E. L. Pollock, *Phys. Rev. Lett.* **56**:351 (1986); E. L. Pollock and D. M. Ceperley, *Phys. Rev. B* **36**:8343 (1987); D. N. Ceperley and E. L. Pollock, *Phys. Rev. B* **39**:2084 (1989).

17. T. A. Kavassalis and J. Noolandi, *Phys. Rev. Lett.* **59**:2674 (1987).
18. P. G. deGennes and J. Matricon, *Mod. Phys.* **36**:45 (1964).
19. R. Labusch, *Phys. Stat. Sol.* **32**:439 (1969).
20. A. L. Fetter, P. C. Hohenberg, and P. Pincus, *Phys. Rev.* **147**:140 (1966).
21. A. Houghton, R. A. Pelcovits, and A. Sudbo, Preprint, Brown University.
22. E. H. Brandt and U. Essman, *Phys. Stat. Sol.* **144**:13 (1987), and references therein.
23. D. Ceperley, G. V. Chester, and M. H. Kalos, *Phys. Rev. B* **17**:1070 (1978).
24. M. Schick, *Phys. Rev. A* **3**:1067 (1971).
25. D. S. Fisher, M. P. A. Fisher, and D. Huse, in preparation.
26. J. W. Elkin, B. Serin, and J. R. Clem, *Phys. Rev. B* **9**:912 (1974).
27. D. Cribier, B. Jacrot, L. M. Rao, and B. Farnoux, *Phys. Rev. Lett.* **9**:106 (1964).
28. R. Wördenweber and P. H. Kes, *Phys. Rev. B* **34**:494 (1986); E. H. Brandt, *Phys. Rev. B* **34**:6514 (1986); *Jap. J. Appl. Phys.* **26**:1515 (1987).